Electronic Supplementary Material (ESI) for Physical Chemistry Chemical Physics.

Ionic Liquid Induced All-α to α+β Conformational Transition in Cytochrome c with Improved Peroxidase Activity in Aqueous Medium

Pankaj Bharmoria,[a] Tushar J Trivedi[b], Anunya Samanta,[c] Ashok Pabbathi,[c] and Arvind Kumar,[*,a,d]

[a]*Academy of Scientific and Innovative research (AcSIR), Central Salt and Marine Chemicals Research Institute, Council of Scientific and Industrial Research (CSIR), G. B. Marg, Bhavnagar-364002, Gujarat, India.*

[b]*Graduate School of EEWS (Energy Environment Water Sustainability), KAIST, 291 Daehak-ro, Yuseong Gu, Daejeon 305-701, Republic of Korea.*

[c]*School of Chemistry, University of Hyderabad, Hyderabad 500 046, India*

[d]*Salt and Marine Chemical Discipline, Central Salt and Marine Chemicals Research Institute, Council of Scientific & Industrial Research (CSIR), G. B. Marg, Bhavnagar-364002, Gujarat, India.*

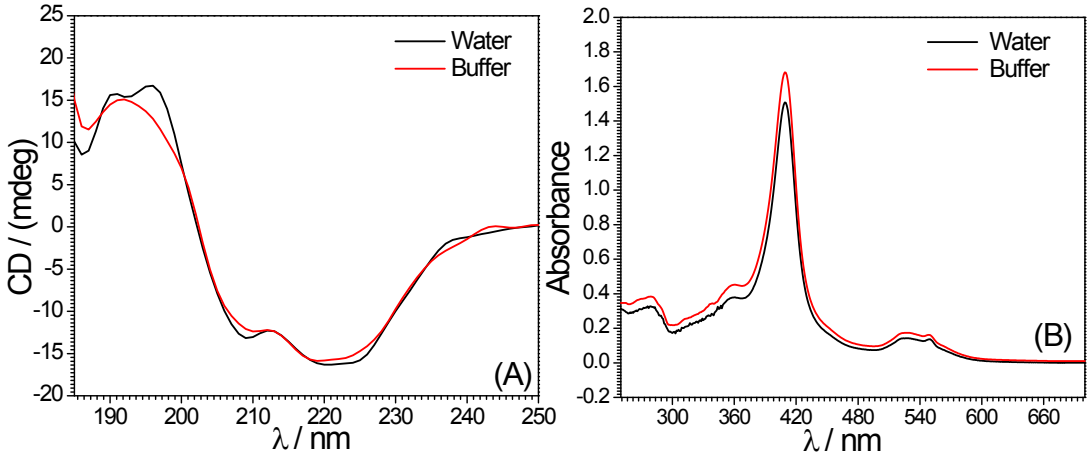

Fig. S1 (A) Far-UV CD spectra of Cyt c (B) UV-Vis-NIR spectra of Cyt c in water and phosphate buffer solution.

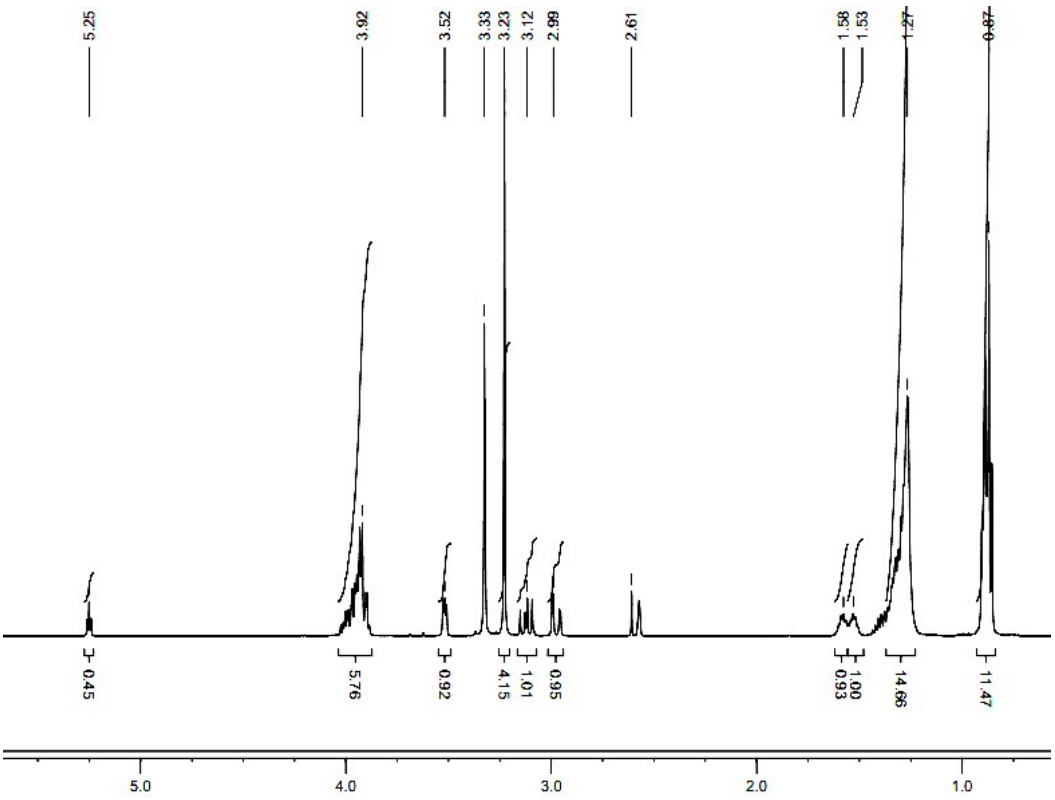

Fig. S2. ^{1}H-NMR: 200MHz (DMSO-d6): δH (ppm) 0.869 (m, 2H), 1.262 (m, 28H), 1.53 (m 2H), 1.58 (m, 2H), 2.98 (m, 2H), 3.116 (m, 2H), 3.228 (s, 9H), 3.519 (m, 2H), 3.92 (m, 2H), 5.25 (t, 1H)

LC-MS Data: ESI-MS: $[C_5H_{14}NO]^+$ m/z:104.14, $[C_{20}H_{37}O_7S]^-$ m/z = 421.2208

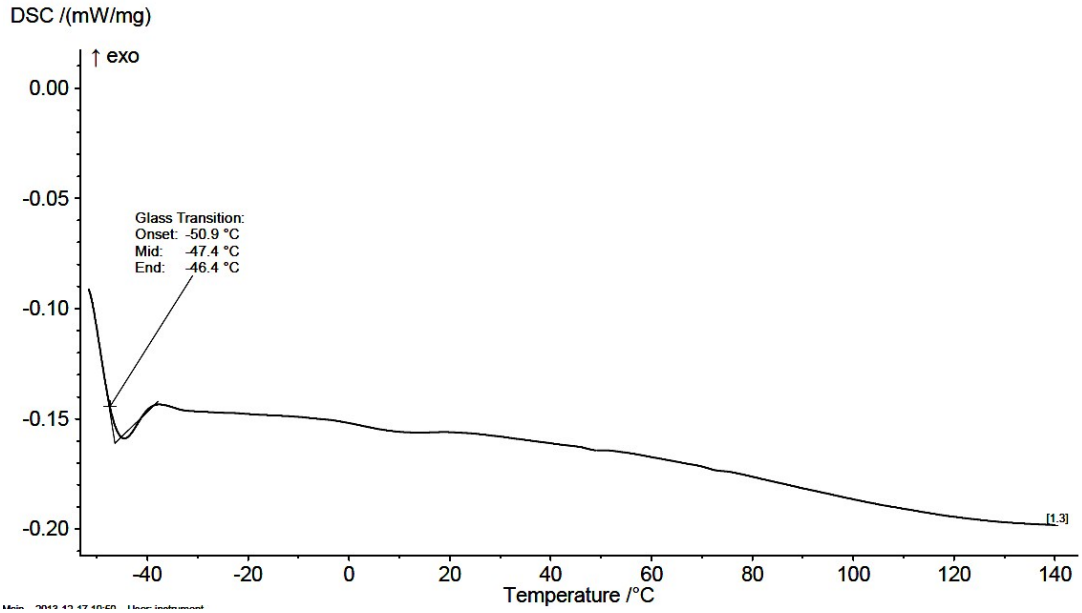

Fig. S3. Differential scanning calorimetric thermogram of native [Cho][AOT].

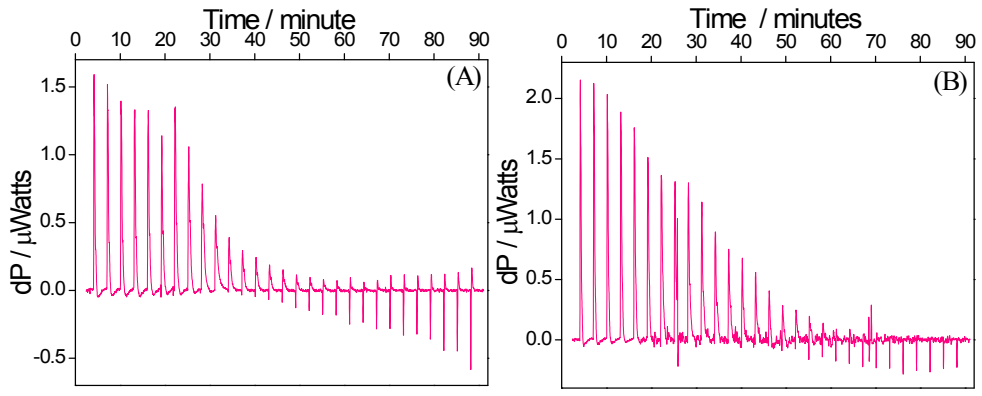

Fig. S4 Differential power (dP) plots of [Cho][AOT] aggregation (A) in buffer and (B) in Cytochrome c solution.

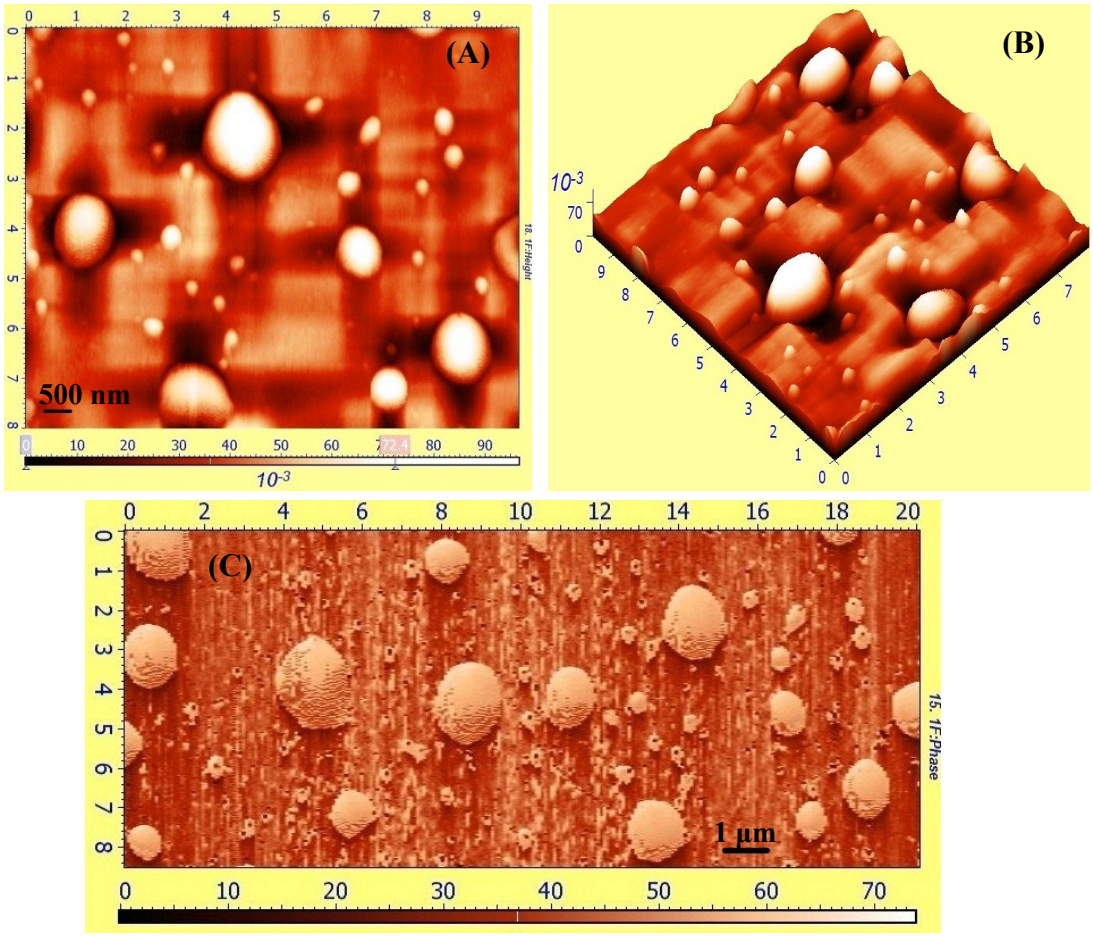

Fig. S5 (A) 2-D (B) 3-D (C) 2-D phase mode AFM images of [Cho][AOT] vesicles in aqueous media. Smaller size vesicles are of the size comparable to that observed from DLS analysis. The larger vesicles are the multiple aggregate vesicles formed by aggregation of smaller vesicles upon sample drying on mica sheet.[1]

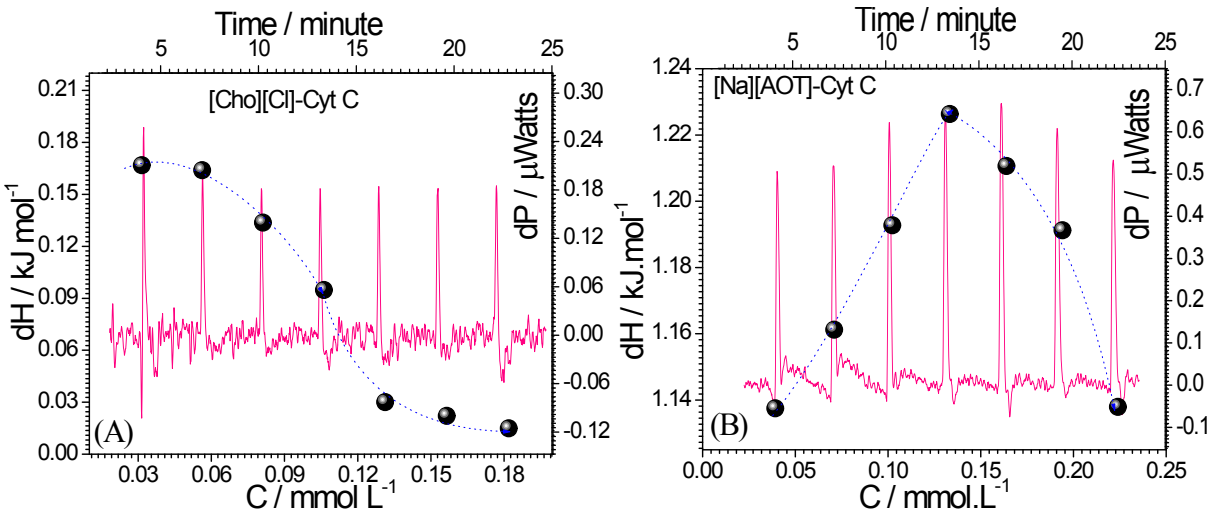

Fig. S6 Binding isotherms of (A) [Cho][Cl] (B) [Na][AOT] to Cyt c solution in low concentration of the salts. Both curves and dP plots are buffer subtracted.

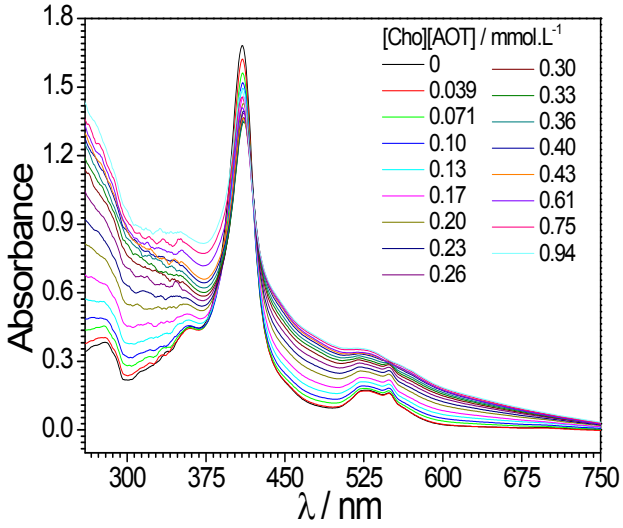

Fig. S7 (A) UV-Vis spectra of Cytochrome c, at different concentrations of [Cho][AOT] showing different absorption wavelengths, 280, 409, 528 and 549 nm.

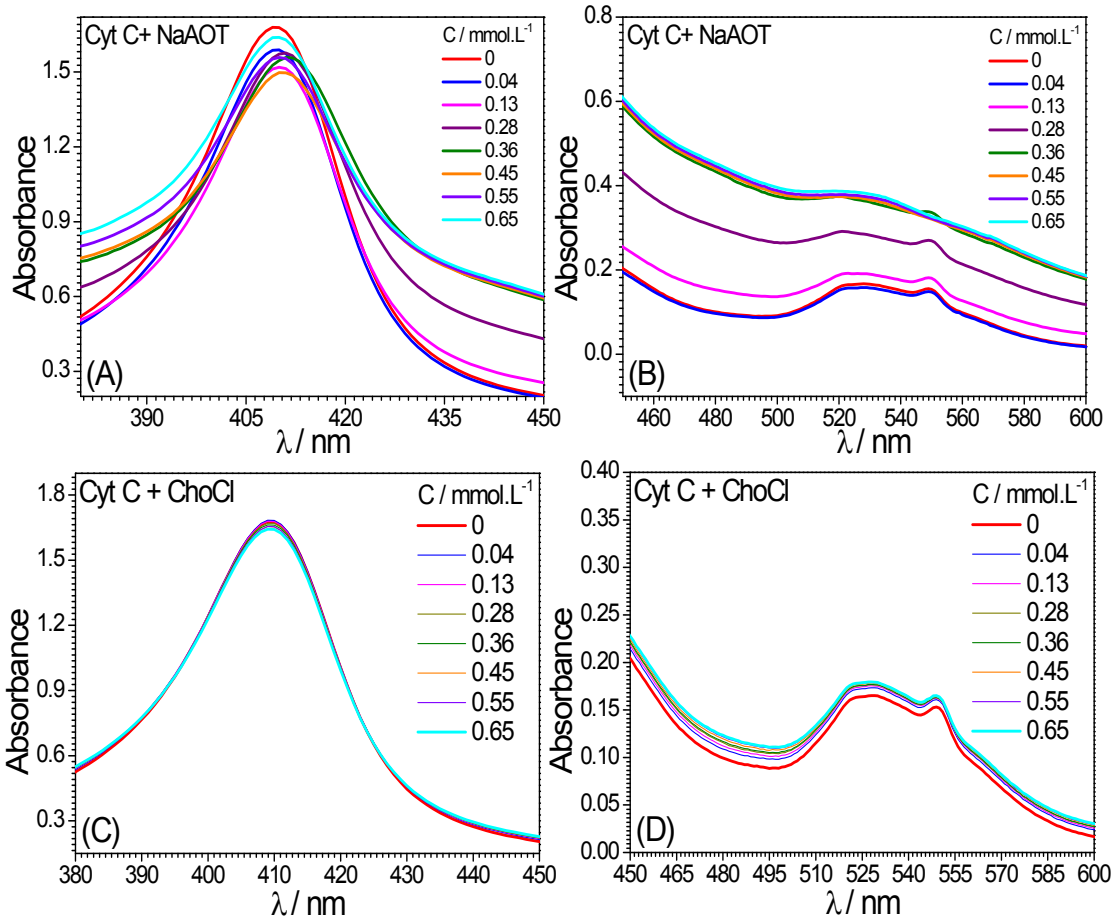

Fig. S8 UV-Vis spectra of Cytochrome c, at different concentrations of (A, B) [Na][AOT] and (C, D) [Cho][Cl] showing different absorption wavelengths, 409, 528 and 549 nm.

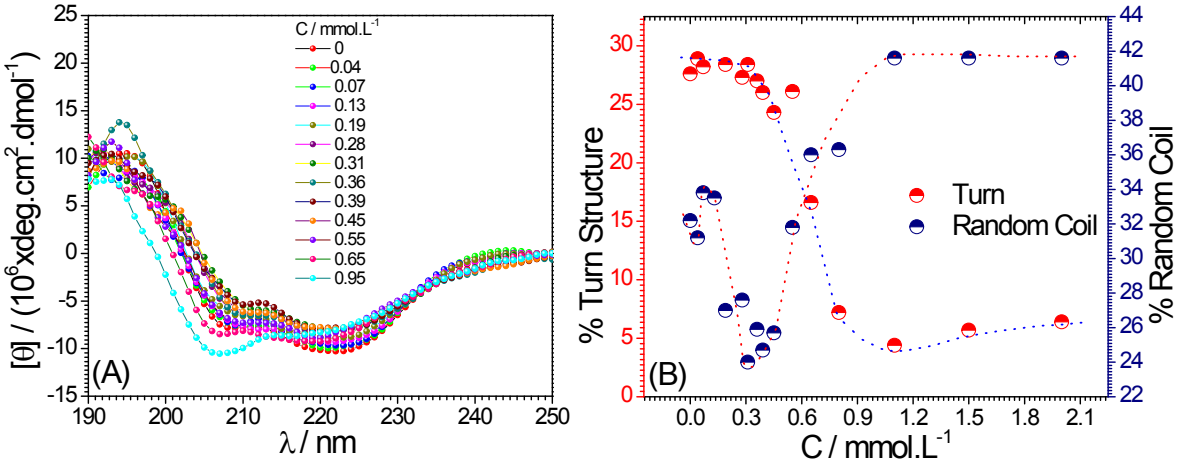

Fig. S9 (A) Far-UV CD spectra of Cytochrome c, at different concentrations of [Cho][AOT] (B) Variation in % turn and % random coil structure of Cyt c.

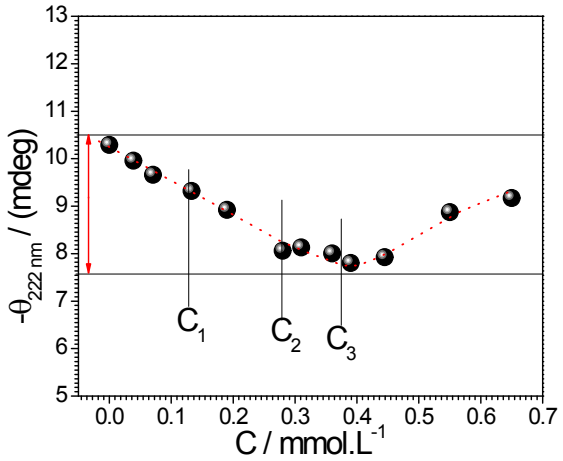

Fig. S10 Changes in the $-\theta_{222\ nm}$ CD peak as a function of [Cho][AOT] concentration.

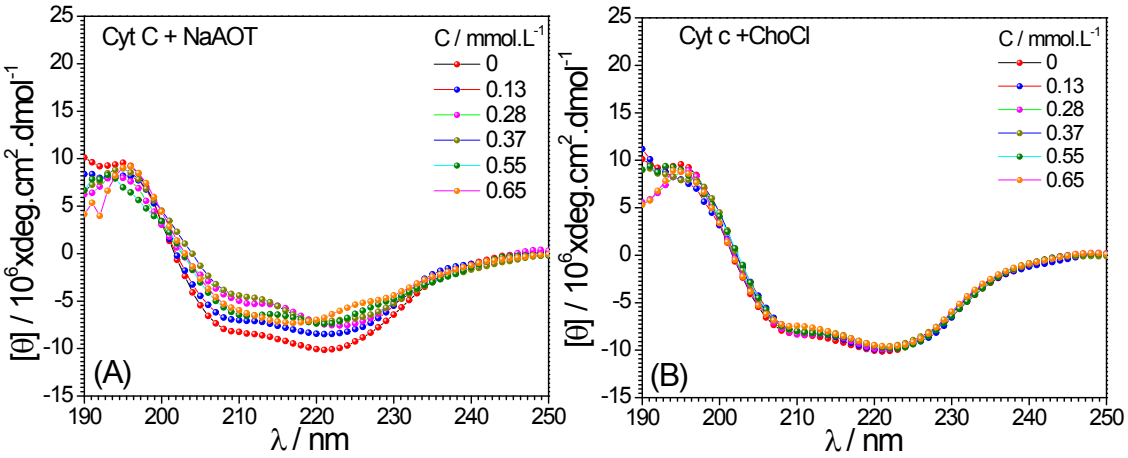

Fig. S11 Far-UV CD spectra of Cytochrome c, at different concentrations of (A) [Na][AOT] and (B) [Cho][Cl].

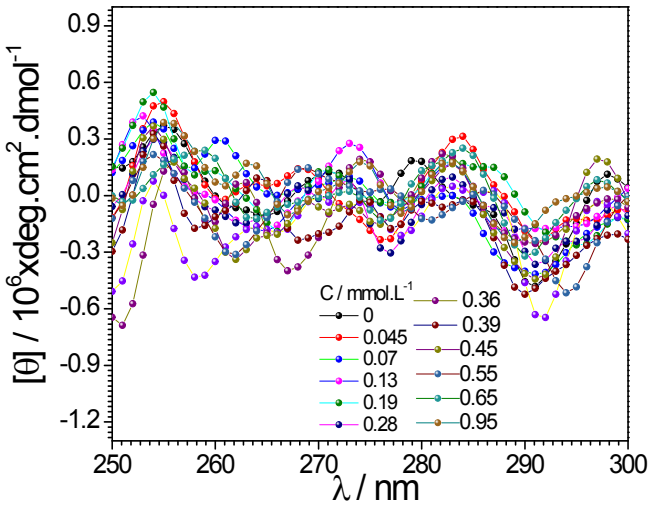

Fig. S12 Mid-UV CD spectra of Cytochrome c, at various concentration of [Cho][AOT]

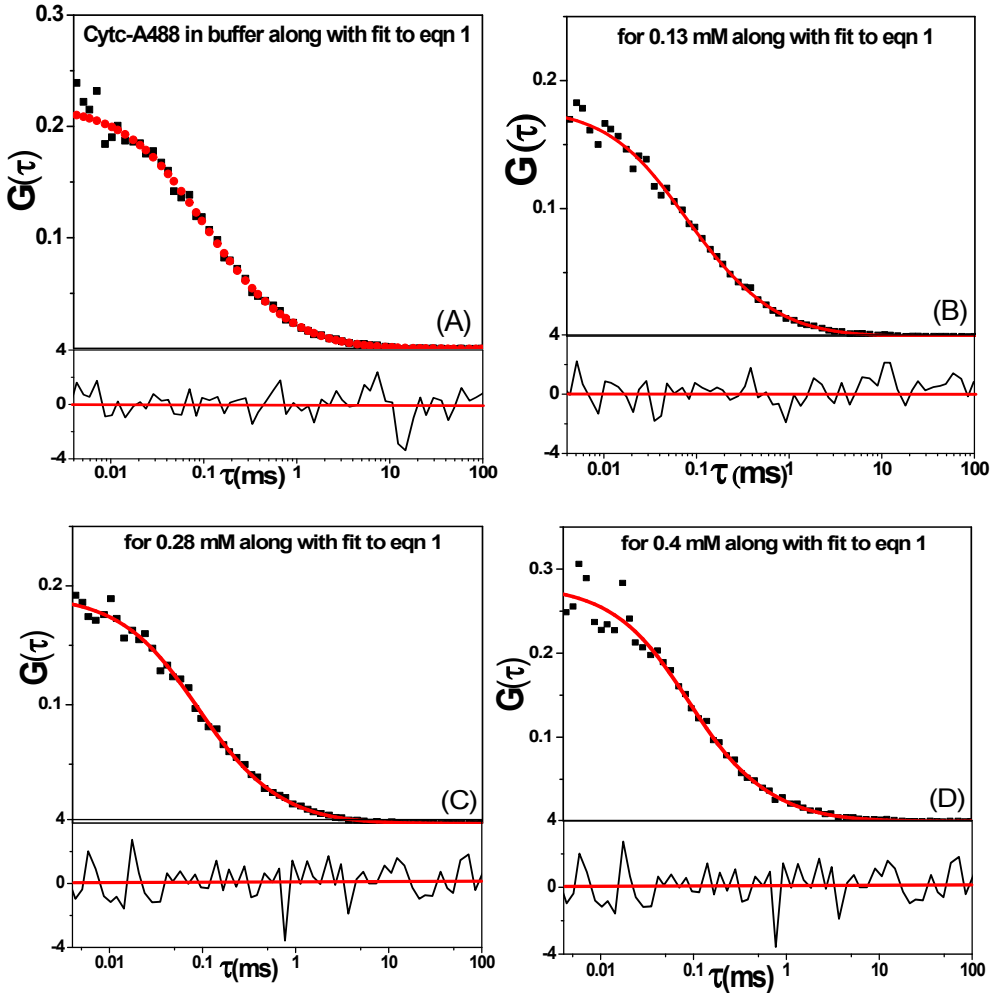

Fig. S13 Correlation data along with fits to single-component diffusion along with conformation fluctuation for A488-Cyt c (A) in phosphate buffer (pH 7.0) and (B) to (D) in [Cho][AOT] solution at varying concentrations from 0.13 mmol.L^{-1} to 0.4 mmol.L^{-1}.

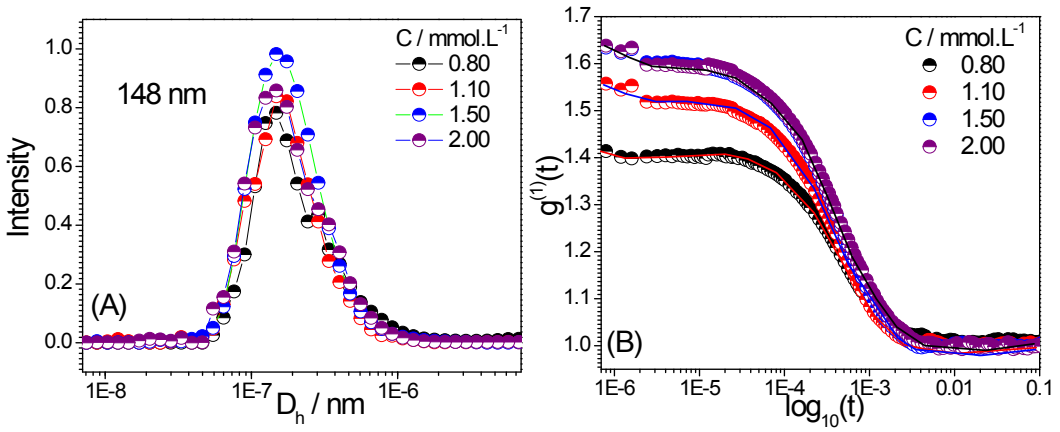

Fig. S14 (A) Hydrodynamic diameter of [Cho][AOT] vesicles at different concentration above CVC (0.4 mmol.L^{-1}) (B) Corresponding first order auto-coorelation functions of [Cho][AOT] vesicles at different concentration.

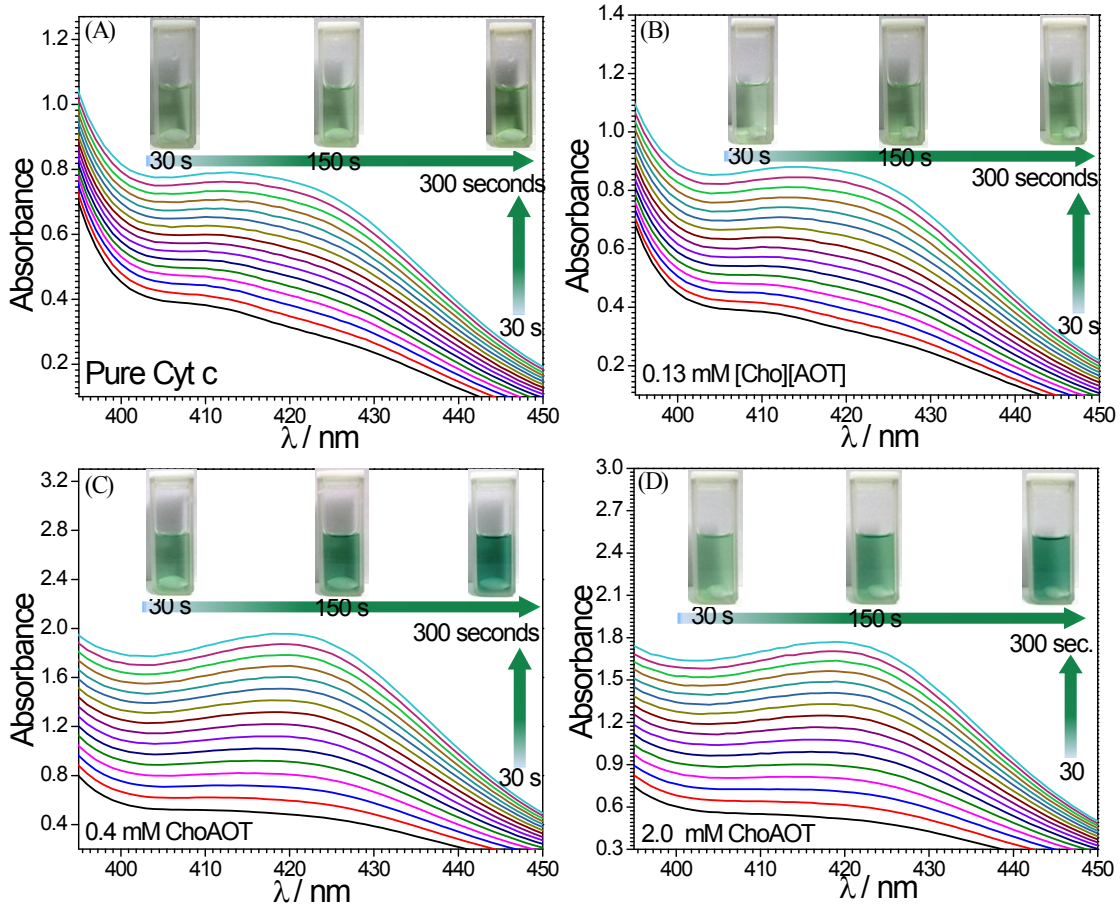

Fig. S15 UV-Vis spectra of ABTS$^{+\bullet}$ at different concentrations of [Cho][AOT]. Images inside the figure showing the color change in reaction mixtures at different time interval.

References:

1. O. Teschke, E. F. de Souza, *Langmuir* **2002,** *18*, 6513-6520.